BOREAL ENVIRONMENT RESEARCH 28: 147–167
ISSN 1797-2469 (online)

Helsinki 5 July 2023

New particle formation in boreal forests of Siberia, Finland and Estonia

Anastasiia Lampilahti[1)*], Olga Garmash[1)†], Mikhail Arshinov[2)], Denis Davydov[2)], Boris Belan[2)], Steffen Noe[3)], Marko Vana[4)], Kaupo Komsaare[4)], Heikki Junninen[4)], Federico Bianchi[1)], Janne Lampilahti[1)], Lubna Dada[1)‡], Veli-Matti Kerminen[1)], Tuukka Petäjä[1)], Markku Kulmala[1)5)6)] and Ekaterina Ezhova[1)**]

[1)] *Institute for Atmospheric and Earth System Research (INAR)/Physics, Faculty of Science, University of Helsinki, Helsinki, P.O.Box 64, 00014, Finland*
*(*corresponding author's e-mail: anastasiia.lampilahti@helsinki.fi)*
*(**corresponding author's e-mail: ekaterina.ezhova@helsinki.fi)*
[2)] *V.E. Zuev Institute of Atmospheric Optics of Siberian Branch of the Russian Academy of Science(IAO SB RAS), Tomsk, 634055, Russia*
[3)] *Institute of Forestry and Engineering, Estonian University of Life Sciences, Tartu, 51006, Estonia*
[4)] *Institute of Physics, Faculty of Science and Technology, University of Tartu, 50411, Tartu, Estonia*
[5)] *Beijing University of Chemical Technology, Beijing, 100029, China*
[6)] *Nanjing University, Nanjing, 210023, China*

[†] *Currently at Department of Atmospheric Sciences, University of Washington, 98195 Seattle, WA, United States*

[‡] *Currently at Laboratory of Atmospheric Chemistry, Paul Scherrer Institute, 5232 Villigen, Switzerland*

Received 4 Aug. 2021, final version received 2 Feb. 2023, accepted 28 Feb. 2023

Lampilahti A., Garmash O., Arshinov M., Davydov D., Belan B., Noe S., Komsaare K., Vana M., Junninen, H., Bianchi F., Lampilahti J., Dada L., Kerminen V.-M., Petäjä T., Kulmala M., & Ezhova E. 2023: New particle formation in boreal forests of Siberia, Finland and Estonia. *Boreal Env. Res.* 28: 147–167.

New particle formation (NPF) is an important atmospheric process where secondary aerosol particles are formed from gas phase precursors. We analyzed the NPF events that were observed in 2016–2018 at three boreal forest stations: the Fonovaya station in Siberia, Russia; the SMEAR II station in Central Finland; and the SMEAR Estonia station in Estonia. NPF events were found to occur less often in Siberia as compared with the European sites. In general, NPF occurred more frequently during daytime under clear sky conditions or in the presence of optically thin clouds, while NPF events were rather rare when the incoming solar radiation was low. Another factor influencing NPF in Siberia is linked to the availability of low-volatility vapors and their precursors. Particularly, a larger number of NPF events was detected under high SO_2 concentrations, indicating the importance of sulfuric acid formed from SO_2. The concentration of SO_2 at the Siberian station is about an order of magnitude higher compared with the two other measurement sites. The concentration of NO_x is also higher at Fonovaya station. During the NPF event days at Fonovaya, the wind was mostly from south-southwest (SSW) and south — the directions associated with the large industrial city Novosibirsk and

Editor in charge of this article: Antti Arola

industrial areas of eastern Kazakhstan. These areas are presumably the main source of anthropogenic trace gases measured at the Fonovaya station. In contrast to the European sites, relative humidity at Fonovaya did not differ significantly between the NPF and non-event days. The condensation sink was higher on non-event days at the European measurement sites but not always at Fonovaya. Air mass back trajectories showed that, oppositely to the European sites, there are no particular sectors around the Siberian site favoring NPF. Our results suggest that solar radiation and subsequent atmospheric chemistry govern the NPF processes in Siberia.

Introduction

Atmospheric new particle formation (NPF) is a phenomenon in which aerosol particles are formed via gas-to-particle conversion (e.g., Kulmala *et al.* 2014). Previous studies have shown that NPF impacts the atmospheric aerosol populations, clouds and potentially climate when the growing fresh particles reach sizes where they can act as cloud condensation nuclei (CCN) (Merikanto *et al.*, 2009; Kazil *et al.*, 2010; Kerminen *et al.* 2012, Gordon *et al.*, 2017; Kalivitis *et al.* 2019). Through aerosol-cloud interactions, aerosol particles may modify many cloud properties, such as their albedo, lifetime, and their impacts on precipitation (e.g., Fan *et al.*, 2016; Rosenfeld *et al.*, 2019; Quaas *et al.*, 2020). NPF occurs in different environments, such as forests, urban areas, polar and coastal regions (Kerminen *et al.* 2018, Chu *et al.* 2019). The boreal forest environment is important for NPF research because NPF is often linked with the emissions of volatile organic compounds (VOCs) from the biosphere (Bäck *et al.* 2012, Tunved *et al.* 2006, Mäki *et al.*, 2019). These VOCs subsequently oxidize into extremely low volatile and low volatility vapors (Kulmala *et al.* 2013, Ehn *et al.* 2014) — precursors of secondary aerosol particles. Boreal forests cover a large area in the Northern Hemisphere, and a dominant fraction of aerosol particles in this environment has been thought to originate from atmospheric NPF during the growing season (Tunved *et al.*, 2006). For observations of atmosphere-biosphere interactions, the network of SMEAR (Station for Measuring Ecosystem–Atmosphere Relations) stations was established initially in boreal forests (Hari and Kulmala, 2005) and more recently in Chinese megacities (Kulmala, 2018).

The frequency of NPF has a considerable spatial and temporal variability across the boreal forest region. As summarized by Kerminen *et al.* (2018) and Artaxo *et al.* (2022), annual NPF event frequencies are typically between 10–30%, with the lowest observed numbers at the northern edge and Siberian part of the boreal forest zone. An exceptionally low NPF frequency was observed at Zotino Tall Tower Facility in central Siberia (Wiedensohler *et al.* 2019), whereas a very high frequency was reported for two sites in western Canada during the summer (Andreae *et al.*, 2022). The frequency of NPF tends to have a spring maximum over boreal forests, sometimes another maximum in late summer or autumn, and a clear winter minimum. Of the sites observed in this paper, the average NPF frequency was reported to be about 26% at the SMEAR II station (Dal Maso *et al.*, 2005, Vana *et al.* 2016, Nieminen *et al.* 2018) and about 21% at the SMEAR Estonia station (Vana *et al.* 2016). The Siberian part of the boreal forest zone is still very poorly characterized in terms of NPF event frequencies.

In general, NPF is controlled by different chemical and physical processes. NPF events are commonly observed in spring and autumn in the boreal forest and have been connected to the forests' biological activity and air mass patterns (Heintzenberg *et al.*, 2011, Nieminen *et al.*, 2018). Winter usually has a clear minimum in NPF events. According to the long-term analyses of the data sets from the SMEAR I and SMEAR II stations, NPF frequency has a considerable interannual variability (Nieminen *et al.*, 2014, Kyrö *et al.*, 2014). At SMEAR II, this variability is connected to air mass transport patterns. At SMEAR I, a decreasing trend of NPF frequency is associated with decreasing sulfur dioxide emissions from the Kola peninsula. Sulfuric acid concentrations, just like organic com-

pounds, play an essential role in the occurrence of NPF (Paasonen *et al.*, 2010; Kulmala *et al.*, 2013).

Although NPF taking place in boreal forests has been studied extensively, many questions remain unanswered. For instance, it is still unclear whether NPF frequencies are generally low in the overall Siberian forests and whether the available studies are representative of the whole region. Furthermore, the drivers and inhibitors behind NPF in Siberia, such as trace gas concentrations, meteorological variables, or air mass transport patterns, have not been studied. Another important question is whether the same precursor vapours, such as sulfuric acid and organic compounds, influence the NPF occurrence in Siberia as in Finland and Estonia. Finally, we need to determine the year-to-year variability of NPF in Siberia and how large-scale effect that is, and whether variability is the same as, for example, at the SMEAR II station.

In order to bridge the knowledge gap outlined above, we performed a comprehensive analysis of the Fonovaya station, similar to the SMEAR II and SMEAR Estonia stations. First, we examined whether NPF in Siberia occurs less often than at the Finnish and Estonian sites. Also, in this analysis, we investigated the connection of NPF with the trace gases O_3, SO_2, and NO_x and with other potentially important parameters, such as the condensation sink (CS), relative humidity (RH), and temperature. Sulfur dioxide is the main source of sulfuric acid vapour, whereas high amounts of NO_x can suppress NPF (Wildt *et al.*, 2014). Ozone is an oxidant that contributes to the production of oxidized organic compounds needed for the growth of newly formed particles (Ehn *et al.*, 2014). Condensation sink describes how rapidly small particles and vapours are scavenged by pre-existing larger particles, so high values of CS decrease the probability of NPF (Kulmala and Kerminen, 2008). Moreover, meteorological variables such as wind speed can also affect NPF. For example, high wind speed can, on the one hand, increase the mixing of condensable compounds and decrease CS promoting NPF or, on the other hand, increase dilution, thus suppressing NPF. Both NPF dynamics have been observed at different sites (Bousiotis *et al.*, 2021). In addition, wind turbulence can enhance NPF via increasing nucleation probability of organic vapors (Kulmala *et al.*, 2023).

In this study, we focus on NPF events at the Fonovaya station located near Tomsk, Russia, and compare our results to those from Finland and Estonia. The main aims are: 1) to test the hypothesis, based on the previous studies, that NPF event frequency is lower in Siberia than at other measurement sites; 2) to characterize NPF observed at the Fonovaya station; and 3) to identify the similarities and differences in the NPF characteristics between these sites. In addition, we aim to understand what research should be performed in the future to identify the reasons behind the rare NPF occurrence in Siberia.

The paper is structured as follows: Materials and methods, description of measurement sites, and instruments used in the experiments are given in the next section. This section is followed by the Results and Discussion section, which contains the classification of NPF events, the effect of solar radiation and trace gases on NPF, and the influence of condensation sink, temperature, and relative humidity on NPF. In addition, the analysis of wind roses and air mass back trajectories is done for the Fonovaya station. Finally, the study's main results are summarized in the last section.

Material and methods

Measurement sites

In this study, we used data sets collected at three stations: the Fonovaya station in West Siberia, located in the Tomsk region, Russia; the SMEAR II station in Hyytiälä, Finland (Hari and Kulmala, 2005); and the SMEAR Estonia station (Noe *et al.*, 2015) in Järvselja, Estonia. The location of the stations is shown in Fig. 1.

The Fonovaya station (56°25′, 84°04′) is located in the boreal forest in West Siberia (Antonovich *et al.*, 2018). The closest city is Tomsk (about 600 000 inhabitants), located 60 km East of the station. Another big city located 170 km SSW from the station is Novosibirsk (1 200 000 inhabitants). The station is located on the river Ob and is surrounded by

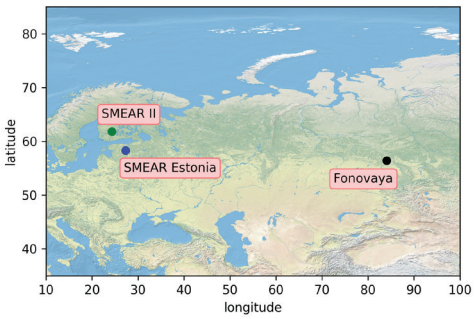

Fig. 1. Location of the three stations.

a mixed forest containing 55-year-old Scots pines (*Pinus sylvestris* L.), 50-year-old birches (*Betula verrucose*), and 32-year-old aspens (*Populus tremula*). The average tree height is 30 m, ranging from about 25 m for the birches to 40 m for the pines. The station monitors meteorological parameters, hourly concentrations of greenhouse and other trace gases and aerosol particles. The observations can be found online at http://lop.iao.ru/EN/.

The SMEAR II station (61°50′, 24°17′) is located in Hyytiälä, southern Finland (Hari and Kulmala, 2005). The closest city is Tampere (around 200 000 inhabitants), based 60 km SW from the station. It is surrounded by a 60-year Scots pine (*Pinus sylvestris* L.) forest, and the average tree height is 18 m. Also, there are several lakes and wetlands around the site. Measurements at the SMEAR II station started in 1996 (e.g., Hari and Kulmala, 2005). More than 1000 parameters are monitored at the SMEAR II station, including meteorological parameters, trace gas concentrations, aerosol characteristics, etc. The data can be found at https://smear.avaa.csc.fi.

The SMEAR Estonia station (58°16′, 27°18′) is established in South East Estonia at the Järvselja Experimental Forestry station (Noe *et al.*, 2015). The closest cities are Tartu (95 000 inhabitants), located 35 km NWW from the station, and Pskov (200 000 inhabitants), located 80 km SE from the station. Mixed forests, lakes, peatlands, and arable lands surround the station. The forest is hemi-boreal and consists of Scots pines (*Pinus sylvestris* L.), Norway spruces (*Picea abies* L.), silver birches (*Betula pendula*) and downy birches (*Betula pubescens*). The stand age is 70 years, on average, ranging from 48-year-old larch stands to 125-year-old pine stands. The average ages are 107 years for the pine, 84 years for the spruce, and 73 years for the birch. The tree height is variable: 22 m on average, varying between 10 and 30 m (Ezhova *et al.*, 2018). At this station, concentrations and fluxes of different parameters in the atmosphere-biosphere system are measured.

At all stations, extensive measurements of aerosol characteristics, greenhouse gases, and trace gases, meteorological parameters are performed. We used the data sets from January 2016 to December 2018; the parameters, corresponding instruments and data availability are summarized in Table 1. The following section discusses the instruments for aerosol measurements in more detail.

Instrumentation

Due to the focus of this study on NPF, here we shortly describe the instruments used for measurements of aerosol particle number size distributions. The number size distributions of particles with diameters from 3 nm to 0.2 μm at the Fonovaya station were measured using a Diffusional Particle Sizer (DPS). The DPS consists of a Novosibirsk-type eight-stage screen diffusion battery (Reischl *et al.*, 1991; Ankilov *et al.*, 2002) connected to the Grimm Condensation Particle Counter (CPC; Model 5.403, GRIMM Aerosol Technik, Germany). The DPS data were inverted to particle size distributions using the algorithm developed by Eremenko and Ankilov (1995), which TSI Inc. chose as the basis for their DPS software (Knutson, 1999). The counting efficiency of ultrafine particles of the CPC mentioned above was considered when calculating size spectra. The distribution of particles in size range from 0.3 μm to 20 μm (15 size bins) was measured by means of the Grimm aerosol spectrometer Model 1.108 (OPC). It was used as a reference instrument during inter-comparison experiments carried out with other optical particle counters (Peters *et al.*, 2006; Sousan *et al.*, 2016; Crilley *et al.*, 2018). For 2016, 80% of data from DPS is available; for 2017 — 81.6% of data, and for 2018 — 94.2%.

Table 1. Instruments and data availability

Fonovaya station		
Parameters	Instrument	Data availability
Particle number size distribution, from 3 nm to 200 nm	Diffusional Particle Sizer (Diffusion Battery + CPC)	85.2%
Particle number size distribution, from 300 nm to 20 μm	Grimm Aerosol Spectrometer Model 1.108	100%
Global solar radiation	Kipp and Zonen CM3 pyranometer	92.6%
Air temperature	Vaisala HMP155	91.9%
Relative humidity		92.1%
Wind velocity	Young Model 85004	91.2%
O_3 concentration	Optec 3.02 P-A	88.4%
NO_2,NO,NO_x concentration	Thermo Scientific Model 42i-TL	91.8%
SO_2 concentration	Thermo Scientific Model 43i-TLE	97.7%
SMEAR II station		
Parameters	Instrument	Data availability
Particle number size distribution, 3 nm to 500 nm	DMPS with Condensation Particle Counters	100%
Global solar radiation	Middleton SK08 (-8/2017) and EQ08 (9/2017-) pyranometer	96%
Air temperature	Pt100 inside custom shield	98.8%
Relative humidity	Rotronic MP102H RH/T sensor	92%
Wind velocity	Thies 2D Ultrasonic anemometer	96.1%
O_3 concentration	TEI 49C	97%
NO_2,NO, NO_x concentration	TEI 42iTL with photolytic converter	97%
SO_2 concentration	TEI 43i-TLE	97.3%
SMEAR Estonia station		
Parameters	Instrument	Data availability
Particle number size distribution, from 2 nm to 40 nm	Neutral cluster and Air Ion Spectrometer (NAIS)	81%
Particle number size distribution, from 3 nm to 10 μm	Electrical Aerosol Spectrometer (EAS)	90%
Global solar radiation	Δ-T SPN1 sunshine pyranometer	100%
Air temperature	Vaisala Weather transmitter WXT520 system	100%
Relative humidity		100%
Wind velocity		100%
O_3 concentration	Thermo Scientific 49i	100%
NO_2,NO, NO_x concentration	Thermo Scientific 42 TL	100%
SO_2 concentration	Thermo Scientific 43i	100%

At the SMEAR II station, aerosol particle number size distribution was measured by a custom-built twin Differential Mobility Particle Sizer system (twin-DMPS, University of Helsinki, Finland) consisting of two Hauke-type differential mobility analyzers (DMA) with closed-loop sheath flow arrangement and two Condensation Particle Counters (CPCs). The first DMPS classifies the particles between 3 and 10 nm and consists of a 10.9-cm-long DMA with a 2mCi Krypton-85 aerosol neutralizer and TSI CPC, model 3025. The second DMPS classifies particles between 10 and 500 nm and consists of a 28-cm-long DMA with a Krypton-85 neutralizer and TSI CPC, model 3010. In total, the twin-DMPS gives a size range from 3 to 500 nm. This DMPS system was described in detail by Aalto *et al.* (2001).

At the SMEAR Estonia station, aerosol particle number size distributions were measured by a Neutral cluster and Air Ion Spectrometer (NAIS, Airel Ltd, Estonia) (Manninen *et al.*, 2009; Mirme and Mirme, 2013.). It contains two DMAs, one of which measures air ions of positive polarity, and the second one measures negative polarity ions. The electric mobility range is from 3.2–0.001 $cm^2 V^{-1} s^{-1}$. Also, the NAIS uses unipolar corona chargers for charging neutral particles to provide measurements of aerosol particles in size range from 2 to 40 nm.

An Electrical Aerosol Spectrometer (EAS, Airel Ltd., Estonia) was also used for measuring the particle number size distribution from 3 nm to 10 μm at SMEAR Estonia. This instrument consists of two multichannel DMAs with 32 measuring channels. For particle charging, unipolar corona chargers are used. It uses different charging mechanisms, such as a weak field ion diffusion mechanism (diffusion charging) and a strong field ion impact mechanism (field charging). Those mechanisms make it possible to detect particles in a wide size range. The instrument was described by Tammet *et al.* (2002) in more detail.

Data analysis

For all data sets, we used the time interval from 11:00 to 16:00 (local time) because the NPF events usually occur in the daytime (Vehkamäki *et al.*, 2004). We focused on spring data because NPF in boreal forests tends to be most frequent in springtime (Kerminen *et al.*, 2018). However, we also investigated the seasonality of NPF. For the trace gases, condensation sink, temperature, relative humidity, and wind speed data sets, we calculated the median values of the spring data for each month separately and compared them between the three stations.

Spatial and temporal variability of the NPF frequency

The classification of NPF events was using the algorithm by Dal Maso *et al.* (2005). According to this classification, NPF event days are defined as those during which a particle burst showing signs of growth is observed. On some days, an apparent and strong particle formation and growth are observed, and these days are identified as Class Ia events. On other days, we observed particle formation with a less clear particle growth; these are classified as Class Ib events. Additionally, there are some days, during which we can identify an NPF event, but the calculation of formation and growth rates (Kulmala *et al.*, 2004) is impossible. Those are classified as Class II events. Events Classes Ia, Ib, II are defined as NPF events in this study. On non-event days, neither formation nor growth of particles nor any nucleation bursts are observed. All other types of events, including "tail", "apple", and "bump" (Buenrostro Mazon *et al.*, 2009; Yli-Juuti *et al.*, 2009), are considered undefined events at all three stations.

We used particle number-size distribution data sets for each station to do classification. Thus, we used DPS data for Fonovaya, DMPS data for SMEAR II, and NAIS data for SMEAR Estonia. The NPF frequency is presented as a fraction of days in a month (NPF days/(NPF days + undefined days + non-event days)). The classification was performed for months with at least 80% of available quality-checked data. Months with a larger amount of bad or missing data were excluded from further analyses.

Sky clearness index

The sky clearness index, P, is a parameter characterizing the incoming shortwave solar radiation. It is equal to the ratio of measured global radiation (R_{meas}) to the theoretical radiation on the top of atmosphere (R_{TOA}) (Dada *et al.*, 2017):

$$P = R_{meas} / R_{TOA}. \quad (1)$$

Theoretical solar radiation at the top of the atmosphere (R_{TOA}) can be calculated by using the following equation:

$$R_{TOA} = I_0 \cos(\mathrm{SZA}), \quad (2)$$

where SZA is solar zenith angle, and I_0 is extraterrestrial solar radiation given by

$$I_0 = \mathrm{TSI}(r_0 / r)^2 \quad (3)$$

Here TSI = 1366 W m^{-2} is total solar irradiance, r is the current Earth-Sun distance, and r_0 is the annual mean distance. I_0 is always within the range of 1321-1415 W m^{-2}. If the clearness index P is close to 1, the sky is clear or covered by optically thin clouds, whereas P approaching 0 corresponds to overcast conditions and optically thick clouds. According to Ylivinkka *et al.* (2020), $P < 0.3$ corresponds to stratocumulus, stratus or nimbostratus clouds, whereas $P > 0.7$ corresponds to a clear sky, cirrus or shallow cumulus clouds. We considered how the NPF frequency depends on the clearness index using events classification and global radiation.

Condensation sink, meteorological parameters and trace gases

We looked at the dependences of NPF events on meteorological parameters (temperature, relative humidity, wind speed), condensation sink, and trace gases (SO_2, NO, NO_2, and O_3). For this, we calculated the median values of all parameters and compared them for: 1) events and non-events at each station; and 2) events between the stations. To compare the median values, we used Wilcoxon rank sum test. Parameter $p < 0.05$ means that there is a statistically significant difference between the median values of the two samples.

We studied the NPF event probability dependence on T and CS for the three stations. For this, we split the temperature and the CS data to bins and for each temperature-CS bin we calculated the NPF event probability as the fraction of NPF event day out of the total number of days in that bin. For those calculations, we took only the data which corresponds to certain clearness index values: $P > 0.76$ for Fonovaya, $P > 0.7$ for SMEAR II and $P > 0.42$ for SMEAR Estonia. The clearness index thresholds were chosen in the way that each plot had approximately 150 data points in total.

Part of the Fonovaya data set was detrended and gapfilled. The raw SO_2 data has an increasing linear trend of the base concentration from 2016 to 2018 related to the instrument calibration. Therefore, we calculated the trend line's slope and removed this trend from the data. For calculating CS at the Fonovaya station, we used combined particle number size distribution from DPS and OPC. In this data set, a 200–300 nm size bin was gap-filled by adding one point with average particle number-size distribution between two neighbouring points (Ezhova *et al.*, 2018). For the SMEAR II station, we used data from DMPS, while for SMEAR Estonia, we used EAS data. The samples are dried at all the sites. In this study, calculated values of the condensation sink were not corrected for particle hygroscopic growth.

Formation and growth rates

The growth rates (GR) of particles during NPF events were calculated for the Fonovaya station. GR is a parameter which describes how fast the particle diameter d_p increases in time during the

$$\mathrm{GR} = \frac{\mathrm{d}d_p}{\mathrm{d}t} = \frac{\Delta d_p}{\Delta t} = \frac{d_{p2} - d_{p1}}{t_2 - t_1}, \quad (4)$$

where d_{p1} and d_{p2} are representative particle diameters at times t_1 and t_2 respectively (Kulmala *et al.*, 2012).

Among several methods for calculating the GRs described by Kulmala *et al.* (2012), the mode fitting method was chosen as the most suitable one. In this method, a log-normal distribution function is fitted with the least square method to the size distribution at each time step. The diameter is then determined as the mode of the log-normal distribution and plotted as a function of time. The resulting GR is the value of the slope of a linear fit to these data points. Here we calculated GRs from 5 to 30 nm.

Particle formation rates (J) during NPF events were calculated for the Fonovaya station. The evolution of particle number concentration dN can be described as:

$$\mathrm{d}N / \mathrm{d}t = \text{production} - \text{losses} = J - \text{losses}. \quad (5)$$

The production term, J, is a parameter that characterizes how fast certain size particles are formed. J can be estimated using the equation (Kulmala *et al.*, 2012):

$$J = \frac{\mathrm{dN}_{dp}}{\mathrm{d}t} + \mathrm{CoagS} \times \mathrm{dN}_{dp} + \frac{\mathrm{GR}}{\Delta d\mathrm{p}} \mathrm{dN}_{dp}, \quad (6)$$

where CoagS is the coagulation sink. This quantity characterizes the removal rate of particles of a specific size due to their collisions with any other larger particles (Dal Maso *et al.*, 2002). The coagulation sink of particles of a diameter, d_p is strongly related to CS (Kulmala *et al.*, 2012), and it can be calculated using the following equation (Kulmala *et al.*, 2012):

$$\mathrm{CoagS}_{dp} = CS \times \left(\frac{d_\mathrm{p}}{0.71} \right)^m, \quad (7)$$

where d_p is given in nm, and the exponent m is about –1.7 (Lehtinen et al, 2007). In this study, we calculated J using the size range, $d\mathrm{N}_{dp}$, of 5 to 30 nm, d_p refers to the lower limit of the size range, and Δd_p — to the size range. For the CoagS, the reference size is 5 nm.

Wind roses and air mass back trajectories

We considered the wind speed at the 40-m height for both NPF event days and non-event days to complement the analysis of the data set from Fonovaya station. Since SO_2 is a precursor for NPF (Lehtipalo *et al.*, 2018, Kulmala *et al.*, 2004, Dada *et al.*, 2020), wind roses were plotted for the SO_2 concentration and wind speed. The wind rose is a way of visualization, which shows how the wind speed or other parameters, in our case SO_2 concentration, depend on the wind direction. Air mass back trajectories were analyzed to study the effects of air mass history on NPF for the Fonovaya station. For this study, we took 96-hour-long back trajectories for spring NPF event days. Each trajectory line represents an air mass that arrived at the station at noon (12:00) at 100 m above the ground level for each NPF event and non-event day during 2016–2018. For this analysis, we used the HYSPLIT (Hybrid Single-Particle Lagrangian Integrated Trajectories) model v.5 with GDAS1 meteorology (Stein *et al.*, 2015). The HYSPLIT model was developed by The National Oceanic and Atmospheric Administration (NOAA) Air Resources Laboratory (ARL). The template Natural Earth I with Shaded Relief, Water, and Drainages (https://www.naturalearthdata.com) was used for data visualization on a map.

Results and Discussion

First, in this section, we present the frequency of the NPF and its interannual variation within the years 2016–2018 at the SMEAR II, SMEAR Estonia and Fonovaya stations. Second, we examine the differences in meteorological parameters and trace gas concentrations between NPF event and non-event days. Then, we shift the main focus onto the Fonovaya station and discuss how wind direction and air mass origin could influence NPF at this site.

Spatial and temporal variability of NPF frequency, formation and growth rates

The seasonal pattern of the frequency of NPF events observed at the SMEAR II station is shown in Fig. 2a. The fraction of both NPF and undefined days was high: 17.2% of all days contained NPF events (see also Table 2), and 36.5% of all days were recognized as undefined

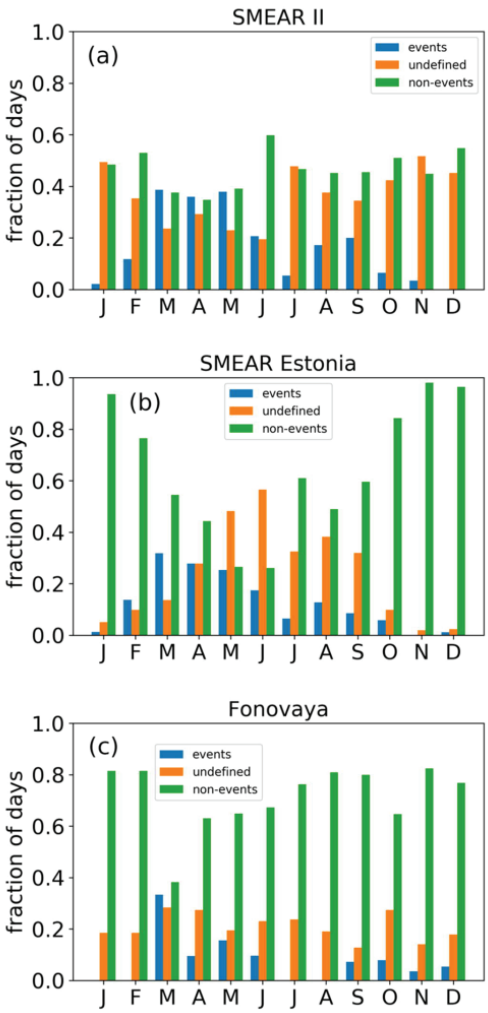

Fig. 2. Monthly fraction of days classified as NPF events, non-events and undefined days for the (**a**) SMEAR II; (**b**) SMEAR Estonia; and (**c**) Fonovaya stations.

ones. In different years, the percentage of NPF event days changed from 10% in 2016 to 23% in 2018. Based on the data set from 1996–2012, NPF events occurred on average 24% of all days at SMEAR II (Nieminen *et al.*, 2018); in 2016–2018, this fraction was somewhat lower due to the seemingly exceptional year 2016, when NPF frequency was only 10% — the lowest number since the beginning of observations.

The frequency of NPF events, non-events, and undefined days at the SMEAR Estonia station is presented in Fig. 2b. NPF events occurred on 13.6% of the days, whereas 21% of the days are classified as undefined days and 65.4% as non-event days. The fraction of NPF and undefined days was lower compared with the SMEAR II station, while the number of non-events was almost 50% higher. A similar research was undertaken by Vana *et al.* (2016) for the data set from 2013–2014. They compared the NPF characteristics at three SMEAR stations: SMEAR II, SMEAR Estonia, and SMEAR I in Värriö, northern Finland. They found that at SMEAR II, NPF events occur on 25% of the days and at SMEAR Estonia — on 20% of the days. In our case, the NPF frequencies were lower by 7–8 percentage points but, similar to the study by Vana *et al.* (2016), the fraction of NPF days was higher at SMEAR II compared with SMEAR Estonia (Table 2). Later, Nieminen *et al.* (2018) reported an average annual NPF frequency of 18% for 2012–2016. The difference in NPF frequencies between the studies can be ascribed either to interannual variability or data availability, which was at 80% both in this study and in Nieminen *et al.* (2018), and 72% in the study by Vana *et al.* (2016). In our case, 20% of missing data lead to the estimate of NPF frequency range of 11–15% (see Supplementary Information), and a similar range

Table 2. Yearly percentage of days, which contain NPF events, non-events and undefined events.

	SMEAR II			
	2016	2017	2018	Total
Events	10.0	18.8	22.8	17.2
Undefined	42.1	30.5	36.8	36.5
Non-events	47.9	50.5	40.4	46.3
	SMEAR Estonia			
	2016	2017	2018	Total
Events	12.2	16.4	12.2	13.6
Undefined	25.2	15.5	22.3	21.0
Non-events	62.6	68.0	65.5	65.4
	Fonovaya			
	2016	2017	2018	Total
Events	10.6	9.3	9.5	9.8
Undefined	18.6	18.1	26.5	21.1
Non-events	70.7	72.5	64.0	69.0

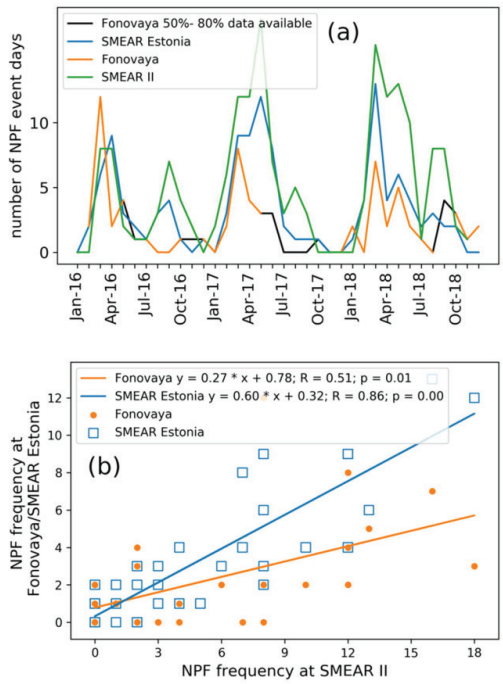

Fig. 3. (**a**) The time series of the monthly number of NPF events at Fonovaya, SMEAR II and SMEAR Estonia. The black line represents frequency for Fonovaya station, where 50–80 % of data are available. (**b**) The correlation of the NPF event days per month between different stations.

based on Nieminen *et al.* (2018) study would be 14.4–19.4%.

According to Vana *et al.* (2016), at SMEAR II and SMEAR Estonia, the fraction of non-event days was similar, about 35% of all the measurement days. Note, however, that a large number of missing days for SMEAR Estonia in that study (30%) could raise the fraction of non-events to 58%, if all these days were non-events. In our study, the fractions of non-event days were 46.3% for SMEAR II and 65.4% for SMEAR Estonia, so our results do not agree with Vana *et al.* (2016) in this respect either due to data issues or a different year range. The seasonal cycle of NPF was studied by Vana *et al.* (2016) who found that the number of NPF event days reaches a maximum in March and a minimum in December–January, with a secondary peak observed in autumn (September–October) at SMEAR Estonia and SMEAR II. Our study produced similar results.

The seasonal pattern of the NPF frequency observed at the Fonovaya station is shown in Fig. 2c. The maximum number of NPF event days was observed in March with comparable values to those at the SMEAR II and SMEAR Estonia stations, but the overall NPF frequency was clearly the lowest (9.8%) among the three stations (Table 2). Undefined days had two maxima, one in spring and another in autumn. Their fraction was 21.1% of all analyzed data, similar to SMEAR Estonia and lower than the corresponding value at SMEAR II. Few NPF events were observed in winter at all three stations.

Figure 3a shows the time series of NPF event days per month for the three stations. The number of event days at the SMEAR II and SMEAR Estonia stations was higher in 2017 and 2018 and lower in 2016. In contrast, the opposite behavior was seen at Fonovaya: the highest number of NPF days was observed in 2016, while in 2017 and 2018, it was lower. However, the amount of missing data (see Table 1) was high at the Fonovaya station in 2017, which could influence this result.

Figure 3b shows the correlation of NPF days per month between the SMEAR II and Fonovaya stations and between the SMEAR II and SMEAR Estonia stations. The pattern of NPF events at the two SMEAR stations closely followed each other, which was confirmed by the high correlation in the number of NPF days per month between these stations ($R = 0.86$). Based on Dal Maso *et al.* (2007), four stations in Finland and Sweden showed similar year-to-year patterns in NPF event frequencies from 2000 to 2004. Our results for the years 2016–2018 suggest that such similarities extend from Nordic areas to Estonia based on the strong correlation between the SMEAR II and SMEAR Estonia data. On the other hand, the correlation between the number of NPF days at the SMEAR II and Fonovaya stations was lower ($R = 0.51$).

Contrasting different boreal environments, NPF events in Siberia were less frequent than in the boreal forests of Finland and Estonia, confirming the findings reported in earlier studies. According to Wiedensohler *et al.* (2019), only 3% of the days displayed an NPF event at the ZOTTO station. Earlier work by Dal Maso

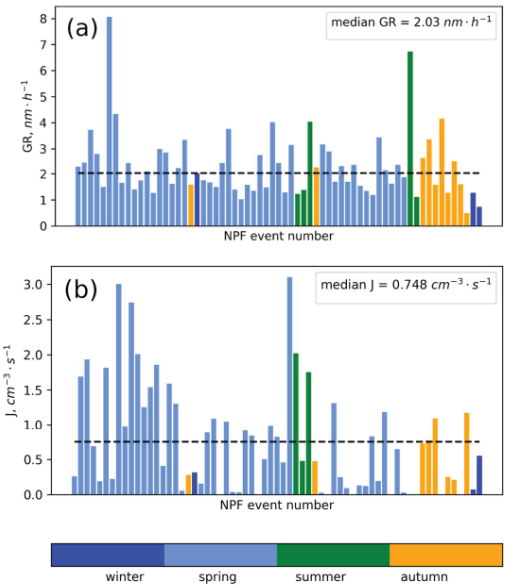

Fig. 4. Growth rate (GR) and formation rate (*J*) at 5–30 nm diameters. Each bar represents the value of GR for a single day when it was possible to calculate (**a**) GR and (**b**) *J*. The dotted line represents the median value for the whole period of measurements. The plots are color-coded seasonally.

et al. (2008) based on one-year data on particle size distributions measured at two stations in Siberia (TOR station in Tomsk and Listvyanka) showed that at both stations, NPF events were observed on 10–12% of the days. This is higher than the results reported for ZOTTO, and agrees with our present results for the Fonovaya station.

To sum up our results on the seasonality of NPF, at all the stations, NPF events were the most frequent in spring, especially in March. This might be connected with the early vegetation period when the plants develop leaves or needles and emit large amounts of VOCs. The overall frequency of NPF event days was the lowest (9.8%) in Siberia, whereas in Finland it was the highest (17.2%) among these three stations. The second maximum of NPF events in August for Finland and Estonia can be connected with senescent plants' emissions (Vermeuel *et al.*, 2022, Hakola *et al.*, 2003). In Estonia and Siberia, there were mostly non-event days in winter, whereas in Finland there were a lot of undefined events in winter.

To characterize NPF events at the Fonovaya station, we calculated the growth rates (GR) of 5–30 nm particles. In Fig. 4a, each bar represents the value of GR for one NPF event day and the color code depicts the seasons. Fig. 4a shows only those days for which it was possible to calculate GRs. More than 70% of the days when the value of GR could be calculated took place in spring. The median GR during the given period of measurements was equal to 2.0 nm h^{-1}. For comparison, the median GRs at the SMEAR II and SMEAR Estonia stations were reported to be equal to 2.1 and 4.6 nm h^{-1}, respectively (Vana *et al.*, 2016). Thus, the typical values of GR seem to be similar between the Fonovaya and SMEAR II stations, whereas at the SMEAR Estonia station they are larger. However, this comparison should be taken with caution due to different years and data from different instruments. This analysis can be continued in future studies.

Particle formation rates (*J*) were also calculated for the Fonovaya station for the NPF days when this calculation was possible (Fig. 4b). The median value of *J* (essentially J_5, as the size range used for calculations was 5–30 nm) during the measurement period (dotted line in Fig. 4b) was equal to 0.75 cm^{-3} s^{-1} (quartiles 0.24–1.26 cm^{-3} s^{-1}). Vana *et al.* (2016) calculated J_3 for the SMEAR II and SMEAR Estonia stations and reported the values of 0.56 and 0.81 cm^{-3} s^{-1}, respectively. Nieminen *et al.* (2018) report formation and growth rates for 10-25 nm size range. Among the events suitable for calculations of *J* and GR, spring data prevails (Fig. 4), we therefore use their spring data for comparison: J_{10} = 1 cm^{-3} s^{-1} and $GR_{10–25}$ = 2.6 nm h^{-1}. These results are reasonably close to ours. A comparison of the particle formation rates at the same size using the data from the same instruments can be done in future studies.

Factors influencing the occurrence of NPF

Effect of solar radiation on NPF

Solar radiation has been found to be perhaps the most important factor for the occurrence of NPF

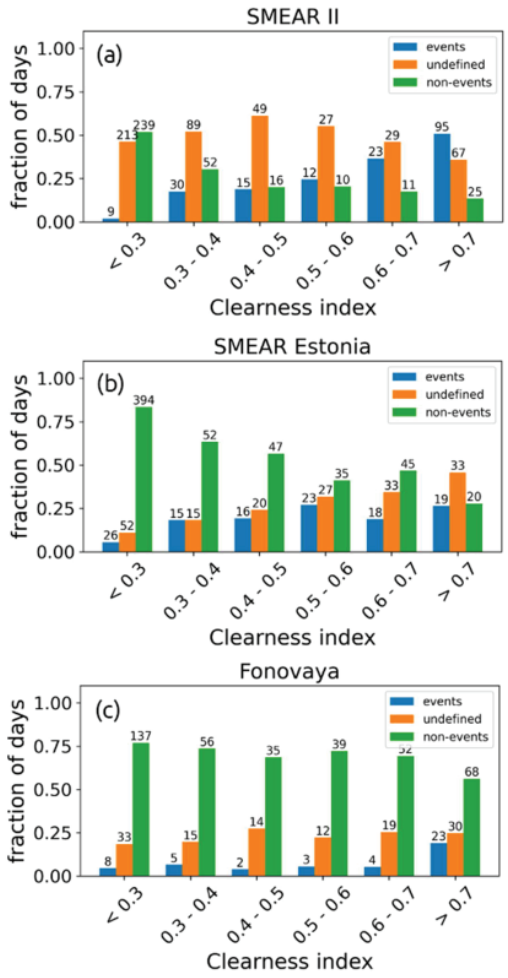

Fig. 5. Fraction of days, classified as NPF events, undefined days and non-events as a function of clearness index for (**a**) SMEAR II, (**b**) SMEAR Estonia and (**c**) Fonovaya stations. The numbers on top of the bars give the total number of days.

(Kerminen *et al.*, 2018). NPF events are more frequent when the clearness index is higher as solar radiation stimulates photochemical processes (Seinfeld and Pandis, 1998; Dada *et al.*, 2017). Figure 5 shows that the frequency of NPF increases with an increasing clearness index P at both SMEAR II and Fonovaya stations. At SMEAR II, NPF events occur on 1% of the days at $P < 0.3$ and 55% at $P > 0.7$ (Table 3; Fig. 5a). The fraction of NPF events at the Fonovaya station (Fig. 5c) was generally lower (19% of all days at $P > 0.7$), but, similarly to SMEAR II, it increased with an increasing clearness index. At SMEAR Estonia, instead, the fraction of undefined days grew from 12% at $P < 0.3$ to 47% at $P > 0.7$, and the fraction of NPF event days did not show any dependence on the clearness index within the range of $P = 0.4$–0.7 (Fig. 5b). Even under high insolation, the fraction of non-event days was high in Siberia: 56% of the days were non-events in comparison to 9% at SMEAR II and 29% at SMEAR Estonia.

To sum up, during the days with optically thick clouds, at $P < 0.3$, NPF events were rarely observed: only about 1-3% of such days contained NPF. Under a clear sky and optically thin clouds, at $P > 0.7$, NPF occurred on 19–55% of the days. These numbers for SMEAR II are similar to the previous analysis of the long-term data set (Dada *et al.*, 2017). Non-event frequency decreased at all three stations with an increasing clearness index. At the same time, simultaneous increases were observed for the NPF event days at SMEAR II and Fonovaya, and the undefined event days at SMEAR Estonia.

Connection of NPF with condensation sink and meteorological parameters

Next, we considered the link between NPF and the following variables: condensation sink (CS), temperature, relative humidity and wind speed. The monthly median values of these parameters are listed in Table 5. Based on our analysis,

Table 3. Percentage of days with events, non-events and undefined events with different values of clearness index.

	SMEAR II		SMEAR Estonia		Fonovaya	
	$P < 0.3$	$P > 0.7$	$P < 0.3$	$P > 0.7$	$P < 0.3$	$P > 0.7$
Events	1%	55%	3%	24%	3%	19%
Undefined	44%	35%	12%	47%	21%	25%
Non-events	53%	9%	85%	29%	76%	56%

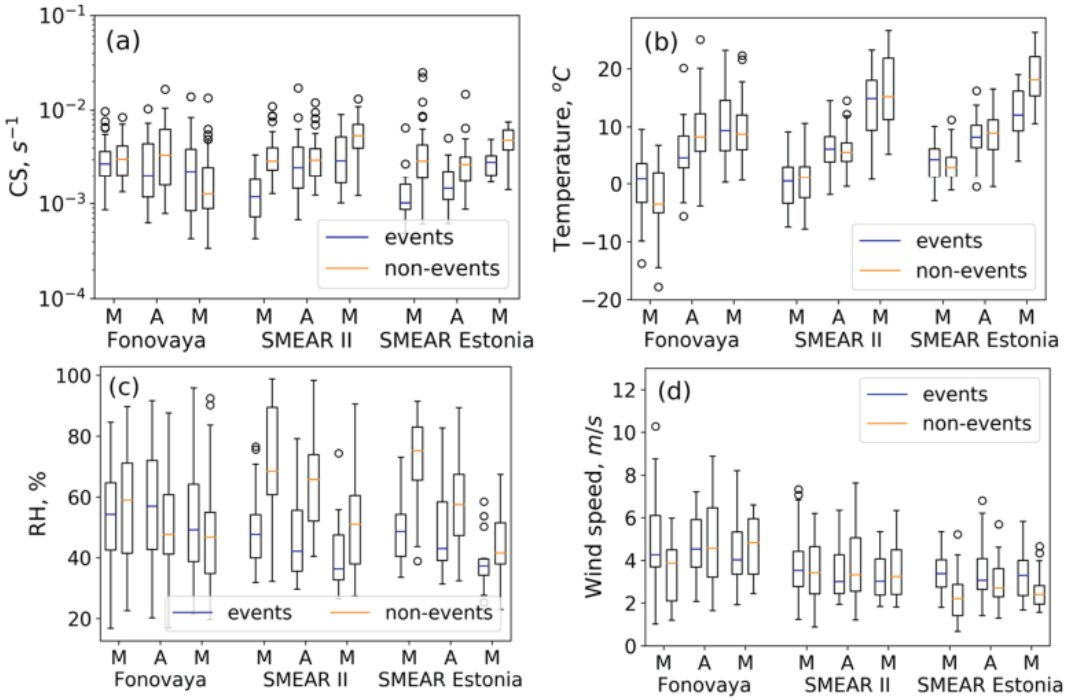

Fig. 6. Box plots for (**a**) condensation sink, (**b**) temperature, (**c**) relative humidity and (**d**) wind speed. The box plots represent numerical data through their median value and quartiles. The box spans the range between the data's 25th to 75th quartile values, with a line at the median value. The whiskers show the most extreme points, which are not outliers. Outliers are marked with circles. The x-axis shows March, April, and May months for each station.

the condensation sink (Fig. 6a, Table 5, and Table S1 in the Supplementary Information) was higher during non-events at all three stations, except in May at the Fonovaya station. However, the difference was statistically significant only at SMEAR stations, and not at Fonovaya (hereafter, all the *p*-values confirming a statistically significant difference between two median values or its absence are reported in Table S1 in the Supplementary Information). In March, the difference in the median CS values between the NPF event and non-event days was a factor of two-three at SMEAR II and SMEAR Estonia, and only 1.12 at Fonovaya. Non-event median values of CS at SMEAR stations are close to those at Fonovaya. Since the highest number of events occurred in March, we can conclude that NPF at Fonovaya generally occurs at larger values of CS as compared with the two SMEAR stations. Furthermore, Kulmala and Kerminen (2008) pointed out that the NPF probability decreases with an increasing CS. In March, CS at Fonovaya on NPF days was 2–3 times higher than at two SMEAR stations, which could be the factor contributing to the lower NPF frequency.

According to our observations, temperature (Fig. 6b) does not influence NPF. At the SMEAR II station, the temperature was almost the same during the NPF event and non-event days (see Table 5). At SMEAR Estonia, the air was somewhat warmer during the NPF events in March (but the temperature difference was not statistically significant) but significantly colder during the NPF events in May. At Fonovaya, the air was warmer during the NPF events in March but colder in April (significant difference). Interestingly, median temperatures during NPF events were similar at SMEAR II and at Fonovaya in March and April, only in May it became warmer at SMEAR II.

Based on the literature (Kerminen *et al.*, 2018), a lower relative humidity (RH) accompanies NPF events at most measurement sites in both clean and polluted environments. In

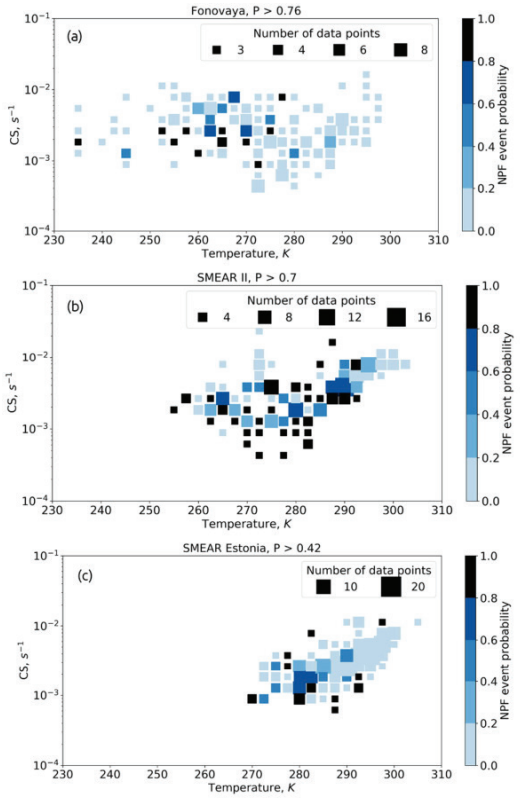

Fig. 7. The NPF event probability in the plane CS — temperature for (**a**) Fonovaya, (**b**) SMEAR II and (**c**) SMEAR Estonia stations. Marker size indicates the number of days included in the probability calculation within each bin.

our data, RH (Fig. 6c, Table 5) was significantly higher during the non-event days at both SMEAR II and SMEAR Estonia. Oppositely, RH did not change much between event and non-event days at Fonovaya (Fig. 6c), likely due to the continental position of the station.

The wind speed was significantly higher during event days in March at SMEAR Estonia but not in other month at any of the stations (Fig. 6d). Thus, wind can be an important factor for NPF at SMEAR Estonia, suggesting that local processes govern atmospheric phenomena on non-event days. In April and May, median winds are approximately 1.5 times stronger at Fonovaya on NPF days as compared with SMEAR stations.

Finally, Fig. 7a, 7b, and 7c show the probability of having a NPF event at the Fonovaya, SMEAR II and SMEAR Estonia stations, respectively, as a function of CS and temperature at 11:00 (temperature representing the intensity of BVOC emissions). At the SMEAR II station, the NPF probability is generally higher, and this conclusion agrees with our previous results (see Spatial and temporal variability of NPF frequency, formation and growth rates section). The lowest NPF probability was observed at Fonovaya. The NPF probability at SMEAR II is higher for low values of CS. At other stations, this difference is not so obvious. At Fonovaya, the temperature range is wider, and the higher event probability is observed for lower temperatures. For SMEAR Estonia, there is an exponential dependence of CS on temperature, which is also observed at other stations above 0°C.

Influence of trace gases on NPF events

Here we analyze the link between NPF events and concentrations of different trace gases (SO_2, NO, NO_2, NO_x, O_3). Similarly to the previous section, we considered their concentrations on NPF event and non-event days (Fig. 8).

For all three stations, the median concentrations of SO_2 were higher on the NPF event days (statistically significant at SMEAR Estonia and Fonovaya, see Table S1 in the Supplementary Information). At the Fonovaya station, the median SO_2 concentration was high: 1.34 ppb during the

Table 4. Median values of concentrations (in ppb) of different trace gases during the NPF event and non-event days in spring (March, April, May) during daytime from 11:00–16:00.

	SO_2	NO_2	NO	O_3
SMEAR II				
Events	0.06	0.21	0.04	42.88
Non-events	0.05	0.475	0.06	40.58
SMEAR Estonia				
Events	0.210	0.522	0.051	44.086
Non-events	0.181	0.683	0.059	40.925
Fonovaya				
Events	1.344	1.889	0.163	24.967
Non-events	0.861	1.460	0.084	23.855

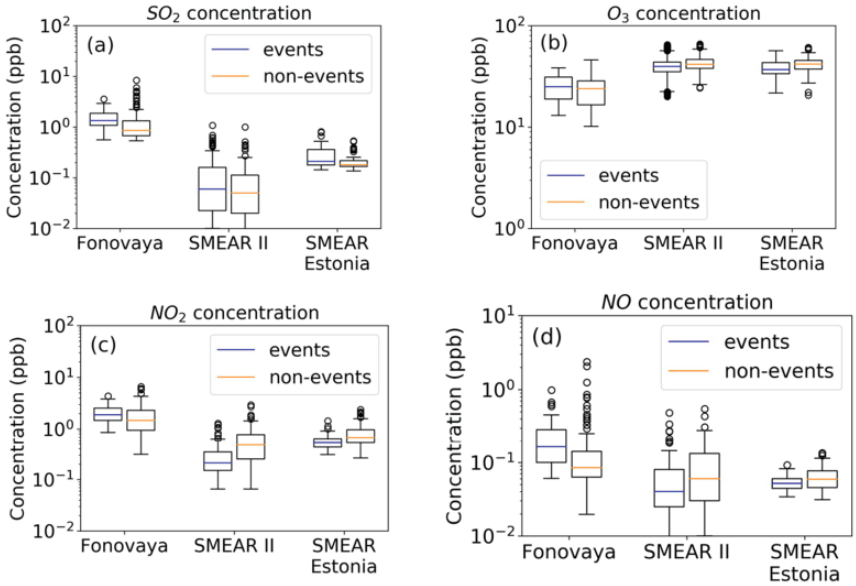

Fig. 8. Concentrations of gases during event and non-event days in spring (March, April, May) for (**a**) SO_2, (**b**) O_3, (**c**) NO_2, and (**d**) NO. For the description of box plots, see the caption to Fig. 6.

Table 5. Monthly median values of condensation sink, temperature, relative humidity and wind speed in spring (March, April, May) during daytime from 11:00–16:00

Site	Month	CS (s^{-1})		Temperature (C)	
		events	non-events	events	non-events
Fonovaya	March	2.71×10^{-3}	3.03×10^{-3}	0.83	–3.57
	April	2.03×10^{-3}	3.34×10^{-3}	4.63	8.22
	May	2.23×10^{-3}	1.26×10^{-3}	9.34	8.74
SMEAR II	March	1.19×10^{-3}	2.90×10^{-3}	0.44	1.10
	April	2.47×10^{-3}	2.96×10^{-3}	6.13	5.58
	May	2.90×10^{-3}	5.37×10^{-3}	14.84	15.17
SMEAR Estonia	March	1.02×10^{-3}	2.08×10^{-3}	4.33	3.00
	April	1.44×10^{-3}	2.65×10^{-3}	8.20	8.93
	May	2.81×10^{-3}	4.79×10^{-3}	12.00	18.08

Site	Month	RH (%)		Wind speed (m/s)	
		events	non-events	events	non-events
Fonovaya	March	54.27	58.92	4.25	3.87
	April	56.90	47.66	4.53	4.56
	May	49.14	46.82	4.02	4.81
SMEAR II	March	47.66	68.42	3.53	3.42
	April	42.13	65.70	3.00	3.32
	May	36.25	50.98	3.01	3.24
SMEAR Estonia	March	48.63	75.10	3.37	2.21
	April	42.95	57.45	3.05	2.70
	May	37.30	41.55	3.29	2.40

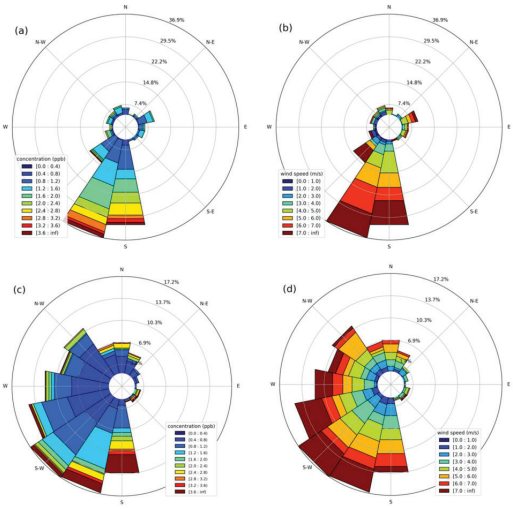

Fig. 9. Wind roses in the spring period (March, April, May) 2017–2019 for the Fonovaya station. Figures show: (**a**) SO_2 concentration during NPF events, (**b**) wind speed during NPF events, (**c**) SO_2 concentration during non-events, and (**d**) wind speed during non-events. The circular format shows the direction of the wind, and the length of each spoke is how often the wind or other parameter occurred from that direction.

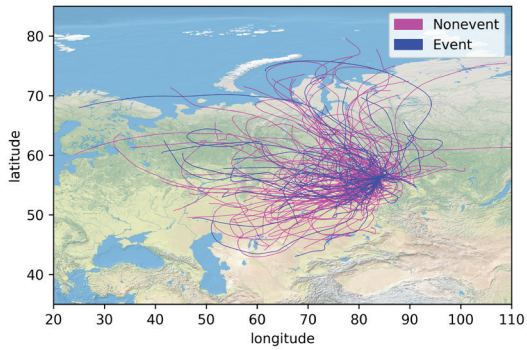

Fig. 10. Air mass back trajectories arriving at Fonovaya during spring at 12:00 (local time) on NPF event and non-event days.

NPF event days, while at SMEAR Estonia this concentration was almost an order of magnitude lower, 0.21 ppb, and at SMEAR II it was even lower at 0.06 ppb (the difference between all stations is statistically significant, see Table S1 in the Supplementary Information).

Our results suggest that the concentration of SO_2 is not a determining factor for NPF events in the boreal forest area: it is highest at Fonovaya, but the NPF frequency is lowest there. This contrasts with findings in more polluted environments. Hamed *et al.* (2010) analysed the dependencies of NPF frequencies at the research station Melpitz, Germany, between two vastly separated time periods: during the 1990s when the SO_2 concentrations were high, and during 2003–2006 when the ambient levels of SO_2 decreased by a factor of ten as a result of social and economic changes. This analysis showed a significant decrease in NPF event frequencies between the two observation periods (–45%). The same result has been shown for polluted environments in both Europe and the USA (Masiol *et al.*, 2018; Saha *et al.*, 2018).

Median concentrations of NO_x at the Fonovaya station were higher than at the two SMEAR stations (Table 4). The concentrations of NO_2 and NO at the Fonovaya station were higher during the NPF event days in comparison to the non-event days (the difference is statistically significant, see Table S1 in the Supplementary Information). This, and similar SO_2 results, indicate that NPF events here are likely associated with anthropogenic influences. In the next section, we analyzed possible sources of trace gases associated with NPF at the Fonovaya station and concluded that the highest concentrations of SO_2 were associated with wind directions from the city of Novosibirsk and Kazakhstan.

At the same time, the median ozone (O_3) concentration at the Fonovaya station was lower than at the SMEAR stations (statistically significant result, see Table S1 in the Supplementary Information), which could be related to higher NOx concentrations there. During the days with NPF events, the median concentrations of ozone were similar at 42.88 ppb and 44.09 ppb for SMEAR II and SMEAR Estonia, respectively, while for Fonovaya, it was 24.97 ppb. Low ozone concentration agrees with the previous studies analyzing ozone mixing ratios in Siberia (Engvall Stjernberg *et al.*, 2012).

Influence of wind direction and air mass transport on NPF at the Fonovaya station

As can be seen from Fig. 8a, the concentration of SO_2 was higher at Fonovaya during the NPF event days. To identify the sources of SO_2

measured at the Fonovaya station, we used wind roses. They illustrate the frequency of cases with different SO_2 concentrations associated with each direction (Fig. 9a, 9c), as well as the wind speed associated with each direction (Fig. 9b, 9d).

Figure 9a and 9c show SO_2 concentration and wind speed for the NPF event days. During these days, the wind blows predominantly from SSW, and the second significant sector is south. To SSW from the Fonovaya station, there is a large industrial city (Novosibirsk), and further to the south an industrial zone of eastern Kazakhstan can be the source of high SO_2 concentrations. The wind speed from the south is higher during the NPF event days in comparison to the non-event days. During the non-event days (Fig. 9c, 9d) the wind is from any direction except the East sector. Usually, the air mass transfer in the region is from the west to the east, in agreement with these wind roses.

To identify the sources of SO_2, we tried to analyze air mass back trajectories using the HYSPLIT model. All 96-hour-long trajectories during the NPF event and non-event days are shown in Fig. 10. It can be seen that the air masses can come from all directions except the SE sector. However, we cannot clearly distinguish sectors associated with NPF event or non-event days, thus it is difficult to conclude what air masses favor NPF processes. This is in contrast to the two SMEAR stations (Vana *et al.*, 2016), where most NPF days are associated with trajectories from the clean northwest sector.

Summary and Conclusions

In this study, we compared characteristics of NPF events observed at three stations: the Fonovaya station in Siberia, Russia; the SMEAR II station in Hyytiälä, Finland; and the SMEAR Estonia station in Järvselja, Estonia, during 2016-2018. Our main aim was to find the differences of NPF characteristics and the factors affecting the occurrence and frequency at the abovementioned stations.

Our results showed that NPF at the Fonovaya station is less frequent than at two other measurement sites in boreal forest environments. Less than 10% of all days at the Fonovaya station contained NPF events, while for SMEAR II this number was 17.2%. At the Fonovaya station, the number of non-event days was the highest at almost 70% of all days. NPF events at all the stations were most frequent in spring, specifically in March, and the second maximum occurred in autumn. Winter was a period of non-event days at both Fonovaya and SMEAR Estonia, whereas at the SMEAR II station many undefined events took place. The particle formation and growth rates at Fonovaya are similar to those obtained by Nieminen *et al.* (2018) and they are similar between the stations.

We investigated the effect of solar radiation on NPF. At both SMEAR II and Fonovaya, the frequency of NPF increased with an increasing clearness index, whereas at the SMEAR Estonia station, the fraction of undefined days increased with an increasing clearness index. At all the measurement sites, NPF events rarely occurred when the clearness index was low (< 0.3) and more often under clear skies or light clouds. Of other meteorological variables, temperature and wind did not obviously affect NPF. The relative humidity and condensation sink were consistently higher during the non-event days at the SMEAR stations, but not at the Fonovaya station.

Further, we investigated the connection of trace gases with NPF in spring. At the Fonovaya station, the median SO_2 concentration was about an order of magnitude higher than at the two SMEAR stations. The median NO_x concentrations were also much higher at Fonovaya in comparison to the SMEAR II and SMEAR Estonia stations. This means that the Fonovaya station is more polluted than the two other measurement sites. The analysis of wind roses showed that during NPF events, the wind blew predominantly from south and south-south-west. The nearest pollution source in that direction is Novosibirsk, which is located 170 km from the station. It can be a source of high SO_2 concentrations at the Fonovaya station. The analysis of air mass back trajectories, however, shows that air masses come from all directions, except south-east, on both NPF event and non-event days. Thus, we did not identify any specific sectors associated with NPF.

Summarizing the results obtained in this study, the frequency of NPF events is the lowest in Siberia and the highest in Finland. The clearness index and concentration of trace gases, especially SO_2, have the largest impact on the Siberian NPF process in spring, less so condensation sink. The relative humidity, temperature and wind speed do not differ between the NPF event and non-event days within the months, but in general, NPF tends to happen at negative or low temperature. In contrast to SMEAR stations, NPF is not related to any clean sector but is associated with elevated levels of SO_2 and NO_x, i.e., anthropogenic pollution. We will continue to investigate the processes influencing NPF in Siberia using the data sets from the new measurement campaign at Fonovaya. For future research, instruments with lower detection limits and higher resolutions are needed. Also, to understand the nature of NPF events in Siberia chemical composition of aerosol particles needs to be measured.

Acknowledgements: We acknowledge financial support from the Academy of Finland Center of Excellence program (grant no. 307331), Academy of Finland professor grant to Markku Kulmala (no. 302958), Academy of Finland Flagship funding (grant no. 337549). ATM-GTP/ERC — European Research Council grant under the European Union's Horizon 2020 research and innovation program (no. 742206), and Jane and Aatos Erkko Foundation. The study was carried out with the financial support of the Russian Foundation for Basic Research (Grant No.19-05-50024) and the Estonian Environmental Investment Centre, the European network for observing our changing planet project (ERA-PLANET, grant agreement no. 689443) under the European Union's Horizon 2020 research and innovation program, Estonian Ministry of Sciences projects (grant nos. P180021, P180274), and the Estonian Research Infrastructures Roadmap project Estonian Environmental Observatory (KKOBS, 3.2.0304.11-0395, 2014-2020.4.01.20-0281). European Regional Development Fund (project MOBTT42), Estonian Research Council (project PRG714, PRG1674) and the European Research Council with the project CHAPAs no. 850614.

Supplementary Information: The supplementary information related to this article is available online at: http://www.borenv.net/BER/archive/pdfs/ber28/ber28-145-167-supplement.pdf

References

Aalto P., Hämeri K., Becker E., Weber R., Salm J., Mäkelä J., Hoell C., O'Dowd C., Hansson H.-C., Väkevä M., Koponen I., Buzorius G. & Kulmala M. 2001. Physical characterization of aerosol particles during nucleation events, *Tellus B*. 53: 344–358.

Andreae M. O., Andreae T. W., Ditas F. & Pöhlker C. 2022. Frequent new particle formation at remote sites in the subboreal forest of North America. *Atmos. Chem. Phys*. 22: 2487–2505.

Ankilov A., Baklanov A., Colhoun M., Enderle K.-H., Gras J, Julanov Yu., Kaller D., Lindner A., Lushnikov A., Mavliev R., McGovern F., Mirme A., O'Connor T., Podzimek J., Preining O., Reischl G., Rudolf R., Sem G., Szymanski W., Tamm E., Vrtala A., Wagner P., Winklmayr W. & Zagaynov V. 2002. Intercomparison of number concentration measurements by various aerosol particle counters. *Atmos. Res.* 62(3–4): 177–207.

Antonovich V.V., Antokhin P.N., Arshinov M.Yu., Belan B.D., Balin Yu. S., Davydov D.K., Ivlev G.A., Kozlov A.V., Kozlov V.S., Kokhanenko G.P., Novoselov M.M., Panchenko M.V., Penner I.E., Pestunov D.A., Savkin D.E., Simonenkov D.V., Tolmachev G.N., Fofonov A.V., Chernov D.G., Smargunov V.P., Yausheva E.P., Paris J.-D., Ancellet G., Law K., Pelon J., Machida T. & Sasakawa M. Station for the comprehensive monitoring of the atmosphere at Fonovaya Observatory, West Siberia: current status and future needs. *Proc. SPIE* 10833, *24th International Symposium on Atmospheric and Ocean Optics: Atmospheric Physics*, 108337Z.

Artaxo P., Hansson H.-C., Andreae M. O., Bäck J., Gomes Alves E., Barbosa H. M. J., Bender F., Bourtsoukidis E., Carbone S., Chi J., Decesari S., Despres BV. R., Ditas F., Ezhova E., Fuzzi S., Hasselquist N. J., Heitzenberg J., Holanda B. A., Guenther A., Hakola H., Heikkinen L., Kerminen V.-M.., Kontkanen J., Krejci R., Kulmala M., Lavric J. V., de Leeuw G., Lehtipalo K., Machado L. A. T., McFiggans G., Franco M. A. M., Meller B. B., Morais F. G., Mohr C., Morgan W., Nilsson M B., Peichl M., Petäjä T., Prass M., Pöhlker C., Pöhlker M. L., Pöschl U., von Randow C., Riipinen I., Rinne J., Rizzo L. V., Rosenfeld D., Silva Dias M. A. F., Sogacheva L., Stier P., Swietlicki E., Sörgel M., Tunved P., Virkkula A., Wang J., Weber B., Yanez-Serrano A. M., Zieger P., Mikhailov E., Smith J. N. & Kesselmeier J. 2022. Tropical and boreal forest-atmosphere interactions: A review. *Tellus B*. 74: 24–163.

Back J., Aalto J., Henriksson M., Hakola H., He Q. and Boy M. 2012. Chemodiversity of a *Scots pine* stand and implications for terpene air concentrations. *Biogeosciences*. 9: 689–702.

Bousiotis D., Brean J., Pope F. D., Dall'Osto M., Querol X., Alastuey A., Perez N., Petäjä T., Massling A., Nøjgaard J. K., Nordstrøm C., Kouvarakis G., Vratolis S., Eleftheriadis K., Niemi J. V., Portin H., Wiedensohler A., Weinhold K., Merkel M., Tuch T. & Harrison R. M. 2021. The effect of meteorological conditions and atmospheric composition in the occurrence and development of new particle formation (NPF) events in Europe. *Atmos. Chem. Phys*. 21: 3345–3370.

Buenrostro Mazon S., Riipinen I., Schultz D.M., Valtanen M., Dal Maso M., Sogacheva L., Junninen H., Nieminen T., Kerminen V.M. & Kulmala M. 2009. Classifying pre-

viously undefined days from eleven years of aerosol-particle-size distribution data from the SMEAR II station, Hyytiälä, Finland. *Atmos. Chem. Phys.* 9: 667–676.

Crilley L.R., Shaw M., Pound R., Kramer L.J., Price R., Young S., Lewis A.C. & Pope F.D. 2018. Evaluation of a low-cost optical particle counter (Alphasense OPC-N2) for ambient air monitoring. *Atmos. Meas. Tech.* 11: 709–720.

Chu B., Kerminen V.M., Bianchi F., Yan C., Petäjä T. & Kulmala M. 2019. Atmospheric new particle formation in China. *Atmos. Chem. Phys.* 19: 115–138.

Dada L., Paasonen P., Nieminen T., Buenrostro Mazon S., Kontkanen J., Peräkylä O., Lehtipalo K., Hussein T., Petäjä T., Kerminen V.M., Bäck J. & Kulmala M. 2017. Long-term analysis of clear-sky new particle formation events and nonevents in Hyytiälä. *Atmos. Chem. Phys.*17: 6227–6241.

Dada L., Lehtipalo K., Kontkanen J., Nieminen T., Baalbaki R., Ahonen L., Duplissy J., Yan C., Chu B., Petäjä T., Lehtinen K., Kerminen V.M., Kulmala M. & Kangasluoma J. 2020. Formation and growth of sub-3–nm aerosol particles in experimental chambers. *Nat. Protoc*. 15: 1013–1040.

Dal Maso M., Kulmala M., Lehtinen K.E., Mäkelä J.M., Aalto P. & O'Dowd C.D. 2002. Condensation and coagulation sinks and formation of nucleation mode particles in coastal and boreal forest boundary layers. *J. Geophys. Res.* 107(D19).

Dal Maso M., Kulmala M., Riipinen I., Wagner R., Hussein T., Aalto P.P. & Lehtinen K.E. 2005. Formation and growth of fresh atmospheric aerosols: eight years of aerosol size distribution data from SMEAR II, Hyytiala, Finland. *Boreal Env. Res*. 10: 323–336.

Dal Maso M., Sogacheva L., Aalto P.P., Riipinen I., Komppula M., Tunved P., Korhonen L., Suur-Uski V., Hirsikko A., Kurten T., Kerminen V.M., Lihavainen H., Viisanen Y., Hansson H.C. & Kulmala M. 2007. Aerosol size distribution measurements at four Nordic field stations: identification, analysis and trajectory analysis of new particle formation bursts. *Tellus B.* 59: 350–361.

Dal Maso M., Sogacheva L., Anisimov M. P., Arshinov M., Baklanov A., Belan B., Khodzher T. V., Obolkin V. A., Staroverova A., Vlasov A., Zagaynov V. A., Lushnikov A., Lyubovtseva Y. S., Riipinen I., Kerminen V.-M. & Kulmala M. 2008. Aerosol particle formation events at two Siberian stations inside the boreal forest. *Boreal Env. Res*. 13: 81–92.

Ehn M., Thornton J.A., Kleist E., Sipilä M., Junninen H., Pullinen I., Springer M., Rubach F., Tillmann R., Lee B., Lopez-Hilfiker F., Andres S., Acir I.H., Rissanen M., Jokinen T., Schobesberger S., Kangasluoma J., Kontkanen J., Nieminen T., Kurten T., Nielsen L.B., Jorgensen S., Kjaergaard H.G., Canagaratna M., Dal Maso M., Berndt T., Petäjä T., Wahner A., Kerminen V.-M., Kulmala M., Worsnop D.R., Wildt J. & Mentel T.F. 2014. A large source of low-volatility secondary organic aerosol. *Nature*. 506: 476–479.

Engvall Stjernberg A.C., Skorokhod A., Paris J.D., Elansky N., Nédélec P. & Stohl A. 2012. Low concentrations of near-surface ozone in Siberia. *Tellus B*. 64: 11607.

Eremenko S. & Ankilov A. 1995. Conversion of the diffusion battery data to particle size distribution: Multiple Solutions Averaging algorithm (MSA). *J. Aerosol Sci.* 26: S749–S750.

Ezhova E., Ylivinkka I., Kuusk J., Komsaare K., Vana M., Krasnova A., Noe S., Arshinov M., Belan B., Park S.B., Lavrič J.V., Heimann M., Petäjä T., Vesala T., Mammarella I., Kolari P., Bäck J., Rannik Ü., Kerminen V.-M. & Kulmala M. 2018. Direct effect of aerosols on solar radiation and gross primary production in boreal and hemiboreal forests. *Atmos. Chem. Phys.* 18: 17863–17881.

Fan J., Wang Y., Rosenfeld D. & Liu X. 2016. Review of aerosol–cloud interactions: Mechanisms, significance, and challenges. *J. Atmos. Sci*. 73: 4221–4252.

Gordon H., Kirkby J., Baltensperger U., Bianchi F., Breitenlechner M., Curtius J., Dias A., Dommen J., Donahue N. M., Dunne E. M., Duplissy J., Ehrhart S., Flagan R. C., Frege C., Fuchs C., Hansel A., Hoyle C. R., Kulmala M., Kürten A., Lehtipalo K., Makhmutov V., Molteni U., Rissanen M. P., Stozhov Y., Tröstl J., Tsakogeorgas G., Wagner R., Williamson C., Wimmer D., Winkler P. M., Yan C. & Carslaw K.S. 2017. Causes and importance of new particle formation in the present-day and preindustrial atmospheres. *J. Geophys. Res. Atmos.* 122: 8739–8760.

Hakola H., Tarvainen V., Laurila T., Hiltunen V., Hellén H., Keronen P. 2003. Seasonal variation of VOC concentrations above a boreal coniferous forest. *Atmos. Environment*. 37: 1623–1634.

Hamed A., Birmili W., Joutsensaari J., Mikkonen S., Asmi A., Wehner B., Spindler G., Jaatinen A., Wiedensohler A., Korhonen H. & Lehtinen K.E.J. 2010. Changes in the production rate of secondary aerosol particles in Central Europe in view of decreasing SO_2 emissions between 1996 and 2006. *Atmos. Chem. Phys.* 10: 1071–1091.

Hari, P. and Kulmala, M. 2005. Station for measuring ecosystem-atmosphere relations (SMEAR II). *Boreal. Env. Res*. 10: 315–322.

Heintzenberg J., Birmili W., Otto R., Andreae M.O., Mayer J.C., Chi X. & Panov A. 2011. Aerosol particle number size distributions and particulate light absorption at the ZOTTO tall tower (Siberia), 2006–2009. *Atmos. Chem. Phys.* 11: 8703–8719.

Kalivitis N., Kerminen V.M., Kouvarakis G., Stavroulas I., Tzitzikalaki E., Kalkavouras P., Daskalakis N., Myriokefalitakis S., Bougiatioti A., Manninen H.E. & Roldin P. 2019. Formation and growth of atmospheric nanoparticles in the eastern Mediterranean: results from long-term measurements and process simulations. *Atmos. Chem. Phys.*19: 2671–2686.

Kazil J., Stier P., Zhang K., Quaas J., Kinne S., O'Donnell D., Rast S., Esch M., Ferrachat S., Lohmann U. & Feichter J. 2010. Aerosol nucleation and its role for clouds and Earth's radiative forcing in the aerosol-climate model ECHAM5–HAM. *Atmos. Chem. Phys.*, 10, 10733–10752.

Kerminen V.M., Paramonov M., Anttila T., Riipinen I., Fountoukis C., Korhonen H., Asmi E., Laakso L., Lihavainen H., Swietlicki E., Svenningsson B., Asmi A.,

Pandis S. N., Kulmala M., & Petäjä, T. 2012. Cloud condensation nuclei production associated with atmospheric nucleation: a synthesis based on existing literature and new results. *Atmos. Chem. Phys.* 12: 12037–12059.

Kerminen V.M., Chen X., Vakkari V., Petäjä T., Kulmala M. & Bianchi F. 2018: Atmospheric new particle formation and growth: review of field observations. *Environ. Res. Lett.* 13(10): 103003.

Knutson, E.O. 1999. History of diffusion batteries in aerosol measurements. *Aeros. Sci. Tech*., 31(2–3): 83–128.

Kulmala M., Vehkamäki H., Petäjä T., Dal Maso M., Ahonen L., Kerminen V.M., Birmili W. & McMurry P.H. 2004. Formation and growth rates of ultrafine atmospheric particles: a review of observations. *J. Aeros. Sci*. 35(2): 143–176.

Kulmala M. & Kerminen V.M. 2008. On the formation and growth of atmospheric nanoparticles. *Atmos. Res.* 90: 132–150.

Kulmala M., Petäjä T., Nieminen T., Sipilä M., Manninen H.E., Lehtipalo K., Dal Maso M., Aalto P.P., Junninen H., Paasonen P. & Riipinen I. 2012. Measurement of the nucleation of atmospheric aerosol particles. *Nat. Protoc*. 7(9): 1651–1667.

Kulmala M., Kontkanen J., Junninen H., Lehtipalo K., Manninen H.E., Nieminen T., Petäjä T., Sipilä M., Schobesberger S., Rantala, P., Franchin, A., Jokinen T., Järvinen E., Äijälä M., Kangasluoma J., Hakala J., Aalto P.P., Mikkilä J., Vanhanen J., Aalto J., Hakola H., Makkonen U., Ruuskanen T., Mauldin III R.L., Duplissy J., Vehkämäki H., Bäck J., Kortelainen A., Riipinen I., Kurten T., Johnston M.V., Smith J.S., Ehn M., Mentel T.F., Lehtinen K.E.J., Laaksonen A., Kerminen V.M. & Worsnop D. 2013. Direct observations of atmospheric aerosol nucleation. *Science*. 339(6122): 943–946.

Kulmala M., Petäjä T., Ehn M., Thornton J., Sipilä M., Worsnop D.R. & Kerminen V.M. 2014. Chemistry of atmospheric nucleation: on the recent advances on precursor characterization and atmospheric cluster composition in connection with atmospheric new particle formation. *Annu. Rev. Phys. Chem.* 65: 21–37.

Kulmala M. 2018. Build a global Earth observatory. *Nature.* 553: 21–23.

Kulmala M., Kokkonen T., Ezhova E., Baklanov A., Mahura A., Mammarella I., Bäck J., Lappalainen H. K., Tyuryakov S., Kerminen V.-M., Zilitinkevich S. & Petäjä T. 2023. Aerosols, Clusters, Greenhouse Gases, Trace Gases and Boundary-Layer Dynamics: on Feedbacks and Interactions. *Boundary-Layer Meteorol*. 186: 475–503.

Kyrö E.M., Väänänen R., Kerminen V.M., Virkkula A., Petäjä T., Asmi A., Dal Maso M., Nieminen T., Juhola S., Shcherbinin A., Riipinen I., Lehtipalo K., Keronen P., Aalto P. P., Hari P. & Kulmala M. 2014. Trends in new particle formation in eastern Lapland, Finland: effect of decreasing sulfur emissions from Kola Peninsula. *Atmos. Chem. Phys.* 14: 4383–4396.

Lehtinen K.E., Dal Maso M., Kulmala M. & Kerminen V.M. 2007. Estimating nucleation rates from apparent particle formation rates and vice versa: Revised formulation of the Kerminen–Kulmala equation. *J. Aeros. Sci*. 38(9): 988–994.

Lehtipalo K., Yan C., Dada L., Bianchi F., Xiao M., Wagner R., Stolzenburg D., Ahonen L., Amorim A., Baccarini A., Bauer P. S. , Baumgartner B., Bergen A., Bernhammer A-K., Breitenlechner M., Brilke S., Buchholz A., Mazon S. B., Chen D., Chen X., Dias A., Dommen J., Draper D. C., Duplissy J., Ehn M., Finkenzeller H., Fischer L., Frege C., Fuchs C., Garmash O., Gordon H., Hakala J., He X., Heikkinen L., Heinritzi M., Helm J. C., Hofbauer V., Hoyle C.R., Jokinen T., Kangasluoma J., Kerminen V-M., Kim C., Kirkby J., Kontkanen J., Kuerten A., Lawler M. J., Mai H., Mathot S., Mauldin R.L., Molteni U., Nichman L., Nie W., Nieminen T., Ojdanic A., Onnela A., Passananti M., Petäjä T., Piel F., Pospisilova V., Quelever L.L.J., Rissanen M.P., Rose C., Sarnela N., Schallhart S., Schuchmann S., Sengupta K., Simon M., Sipilä M., Tauber C., Tome A., Trostl J., Väisänen O., Vogel A.L., Volkamer R., Wagner A.C., Wang M., Weitz L., Wimmer D., Ye P., Ylisirniö A., Zha Q., Carslaw K.S., Curtius J., Donahue N. M., Flagan R.C., Hansel A., Riipinen I., Virtanen A., Winkler P. M., Baltensperger U., Kulmala M. & Worsnop D. R. 2018. Multicomponent new particle formation from sulfuric acid, ammonia, and biogenic vapors. *Science Advances.* 4(12): p.eaau5363.

Mäki M., Aaltonen H., Heinonsalo J., Hellén H., Pumpanen J. & Bäck, J. 2019. Boreal forest soil is a significant and diverse source of volatile organic compounds. *Plant and Soil.* 441:89–110.

Manninen H.E., Petäjä T., Asmi E., Riipinen I., Nieminen T., Mikkilä J., Hõrrak U., Mirme A., Mirme S., Laakso L. & Kerminen V.M. 2009. Long-term field measurements of charged and neutral clusters using Neutral cluster and Air Ion Spectrometer (NAIS). *Boreal Env. Res*. 14: 591–605.

Masiol M., Squizzato S., Chalupa D.C., Utell M.J., Rich D.Q. & Hopke P.K. 2018. Long-term trends in submicron particle concentrations in a metropolitan area of the northeastern United States. *Sci. Total Environ*., 633: 59–70.

Merikanto J., Spracklen D.V., Mann G.W., Pickering S.J. & Carslaw K.S. 2009. Impact of nucleation on global CCN. *Atmos. Chem. Phys.* 9: 8601–8616.

Mirme S. & Mirme A. 2013. The mathematical principles and design of the NAIS–a spectrometer for the measurement of cluster ion and nanometer aerosol size distributions. *Atmos. Meas. Tech.* 6: 1061–1071.

Nieminen T., Kerminen V.M., Petäjä T., Aalto P.P., Arshinov M., Asmi E., Baltensperger U., Beddows D., Beukes J.P., Collins D., Ding,A. Harrison R. M., Henzing B., Hooda R., Hu M., Hõrrak U., Kivekäs N., Komsaare K., Krejci R., Kristensson A., Laakso L., Laaksonen A., Leaitch W. R., Lihavainen H., Mihalopoulos N., Németh Z., Nie W., O'Dowd C., Salma I., Sellegri K., Svenningsson B., Swietlicki E., Tunved P., Ulevicius V., Vakkari V., Vana M., Wiedensohler A., Wu Z., Virtanen A. & Kulmala M. 2018. Global analysis of continental boundary layer new particle formation based on long-term measurements. *Atmos. Chem. Phys.* 18: 14737–14756.

Nieminen T., Asmi A., Dal Maso M., Aalto, P.P., Keronen

P., Petäjä T., Kulmala M. and Kerminen V.M. 2014. Trends in atmospheric new-particle formation: 16 years of observations in a boreal-forest environment. *Boreal Env. Res*. 19B: 191–214.

Noe S.M., Niinemets Ü., Krasnova A., Krasnov D., Motallebi A., Kängsepp V., Jõgiste K., Hõrrak U., Komsaare K., Mirme S. & Vana M. 2015. SMEAR Estonia: Perspectives of a large-scale forest ecosystem–atmosphere research infrastructure. *Forestry Studies*. 63(1): 56–84.

Paasonen P., Nieminen T., Asmi E., Manninen H.E., Petäjä T., Plass-Dülmer C., Flentje H., Birmili W., Wiedensohler A., Hõrrak U., Metzger A. Hamed A., Laaksonen A., Facchini M. C., Kerminen V.-M. & Kulmala M. 2010. On the roles of sulphuric acid and low-volatility organic vapours in the initial steps of atmospheric new particle formation. *Atmos. Chem. Phys.* 10: 11223–11242.

Peters T.M., Ott D. & O'Shaughnessy P.T. 2006. Comparison of the Grimm 1.108 and 1.109 portable aerosol spectrometer to the TSI 3321 aerodynamic particle sizer for dry particles. *Ann. Occup. Hyg.* 50(8): 843–850.

Quaas J., Arola A., Cairns B., Christensen M., Deneke H., Ekman A.M., Feingold G., Fridlind A., Gryspeerdt E., Hasekamp O., Li Z., Lipponen A., Ma P.-L., Mülmenstädt J., Nenes A., Penner J. E., Rosenfeld D., Schrödner R., Sinclair K., Sourdeval O., Stier P., Tesche M., van Diedenhoven B. & Wendisch M. 2020. Constraining the Twomey effect from satellite observations: issues and perspectives. *Atmos. Chem. Phys.* 20: 15079–15099.

Reischl G.P., Majerowicz A., Ankilow A., Eremenko S. & Mavliev R. 1991. Comparison of the Novosibirsk automated diffusion battery with the Vienna electro mobility spectrometer. *J. Aeros. Sci.* 22: 223–228.

Rosenfeld D., Zhu Y., Wang M., Zheng Y., Goren T. & Yu S. 2019. Aerosol-driven droplet concentrations dominate coverage and water of oceanic low-level clouds. Science. 363: eaav0566.

Saha P.K., Robinson E.S., Shah R.U., Zimmerman N., Apte J.S., Robinson A.L. & Presto A.A. 2018. Reduced ultrafine particle concentration in urban air: changes in nucleation and anthropogenic emissions. *Environ. Sci. Tech.* 52: 6798–6806.

Seinfeld J.H. & Pandis S.N. 2016. Atmospheric Chemistry and Physics: From Air pollution To Climate Change. John Wiley & Sons. 1120 p.

Sousan S., Koehler K., Hallett L. & Peters T.M. 2016. Evaluation of the Alphasense optical particle counter (OPC-N2) and the Grimm portable aerosol spectrometer (PAS-1.108). *Aeros. Sci. Tech.* 50: 1352–1365.

Stein A.F., Draxler R.R., Rolph G.D., Stunder B.J., Cohen M.D. and Ngan, F. 2015. NOAA's HYSPLIT atmospheric transport and dispersion modeling system. *Bull. Am. Meteorol. Soc.* 96: 2059–2077.

Tammet H., Mirme A. & Tamm E. 2002. Electrical aerosol spectrometer of Tartu University. *Atmos. Res*. 62(3–4): 315–324.

Tunved P., Hansson H.C., Kerminen V.M., Ström J., Dal Maso, M., Lihavainen H., Viisanen Y., Aalto P.P., Komppula M. & Kulmala M. 2006. High natural aerosol loading over boreal forests. *Science*. 312: 261–263.

Vana M., Komsaare K., Hõrrak U., Mirme S., Nieminen, T., Kontkanen, J., Manninen, H.E., Petäjä T., Noe S.M. & Kulmala M. 2016. Characteristics of new-particle formation at three SMEAR stations. *Boreal Env. Res*. 21: 345 - 362.

Vehkamäki H., Dal Maso M., Hussein T., Flanagan R., Hyvärinen A., Lauros J., Merikanto P., Mönkkönen M., Pihlatie K., Salminen K., Sogacheva L., Thum T., Ruuskanen T. M., Keronen P., Aalto P. P., Hari P., Lehtinen,K. E. J., Rannik Ü. & Kulmala M. 2004. Atmospheric particle formation events at Värriö measurement station in Finnish Lapland 1998–2002. *Atmos. Chem. Phys.* 4: 2015–2023.

Vermeuel M. P., Novak G. A., Kilgour D. B., Claflin M. S., Lerner B. M., Trowbridge A. M., Thom J., Cleary P. A., Desai A. R. & Bertram T. H. 2023. Observations of biogenic volatile organic compounds over a mixed temperate forest during the summer to autumn transition. *Atmos. Chem. Phys.* 23: 4123–4148.

Wiedensohler A., Ma N., Birmili W., Heintzenberg J., Ditas F., Andreae M.O. & Panov A. 2019. Infrequent new particle formation over the remote boreal forest of Siberia. *Atmos. Environment*. 200: 167–169.

Wildt J., Mentel T.F., Kiendler-Scharr A., Hoffmann T., Andres S., Ehn M., Kleist E., Müsgen P., Rohrer F., Rudich Y., Springer M., Tillmann R. & Wahner A. 2014. Suppression of new particle formation from monoterpene oxidation by NOx. *Atmos. Chem. Phys.* 14: 2789–2804.

Yli-Juuti T., Riipinen I., Aalto P.P., Nieminen T., Maenhaut W., Janssens I.A., Claeys M., Salma I., Ocskay R., Hoffer A., Imre K. & Kulmala M. 2009. Characteristics of new particle formation events and cluster ions at K-puszta, Hungary. *Boreal Environ. Res.*14:683–698.

Ylivinkka I., Kaupinmäki S., Virman M., Peltola M., Taipale D., Petäjä T., Kerminen V.M., Kulmala M. & Ezhova E. 2020. Clouds over Hyytiälä, Finland: an algorithm to classify clouds based on solar radiation and cloud base height measurements. *Atmos. Meas. Tech.* 13: 5595–5619.